The 2005 HST Calibration Workshop
Space Telescope Science Institute, 2005
A. M. Koekemoer, P. Goudfrooij, and L. L. Dressel, eds.

Spectral Extraction of Extended Sources Using Wavelet Interpolation

Paul Barrett

Department of Physics and Astronomy, Johns Hopkins University, Baltimore, MD 21218

Linda L. Dressel

Space Telescope Science Institute, Baltimore, MD 21218

Abstract. Spatially-resolved spectroscopic investigations of extended sources using STIS, such as galactic black hole mass measurements and chemistry in spatially resolved structures around Eta Carinae, use a narrow extraction width (1-2 pixels wide) to minimize source confusion. However, the combination of the finite pixel size of the CCD and the slight tilt of the spectrum cause problems for the CALSTIS extraction algorithm, resulting in spectra having a scalloped pattern (i.e. aliasing). A wavelet interpolation algorithm is presented that nearly eliminates aliasing, while preserving the flux content of the subpixels. This algorithm will be implemented as a STSDAS task.

1. Introduction

Spatially-resolved spectroscopic investigations of extended sources using the Space Telescope Imaging Spectrograph (STIS), such as galactic black hole mass measurements (Dressel 2003) and chemistry in spatially resolved structures around Eta Carinae (Davidson 2004), use a narrow extraction mask (1-2 pixels wide) to minimize source confusion. However, the narrow mask causes the spectra to show a scalloped pattern (Figure 1). This strong ($\sim 15\%$) aliasing is due to the point spread function (PSF) being only marginally sampled (FWHM ~ 1.3 pixels) and the spectral trace (i.e. the peak or ridge of the spectrum) being slightly tilted with respect to the rows of the detector (Figure 2). For point-source spectra, a mask with a large (7 pixels for CCD modes) extraction width is used, which encompasses all of the flux and avoids the aliasing problem. To minimize aliasing, the STIS Instrument Handbook (Kim Quijano et al. 2003) recommends dithering spectral observations along the slit by a half pixel. This is often not done, because it doubles the requested exposure time, perhaps resulting in a less competitive proposal. When done, it reduces the magnitude of the aliasing, but also doubles its frequency, which can be problematic for spectral features of comparable scale. This paper describes a wavelet interpolation algorithm that nearly eliminates the aliasing problem for narrow extraction masks, while preserving the flux content of the interpolated spectral image.

2. Average Interpolation

Interpolation is widely used in the calibration and analysis of astronomical data to transform images to a common frame or uniform grid. The most commonly used algorithms are linear and bi-linear interpolation for one- and two-dimensional data, respectively. These simple algorithms are usually sufficient for a rough estimate of the interpolated value, but can give erroneous results when high precision is needed. This is particularly true when the

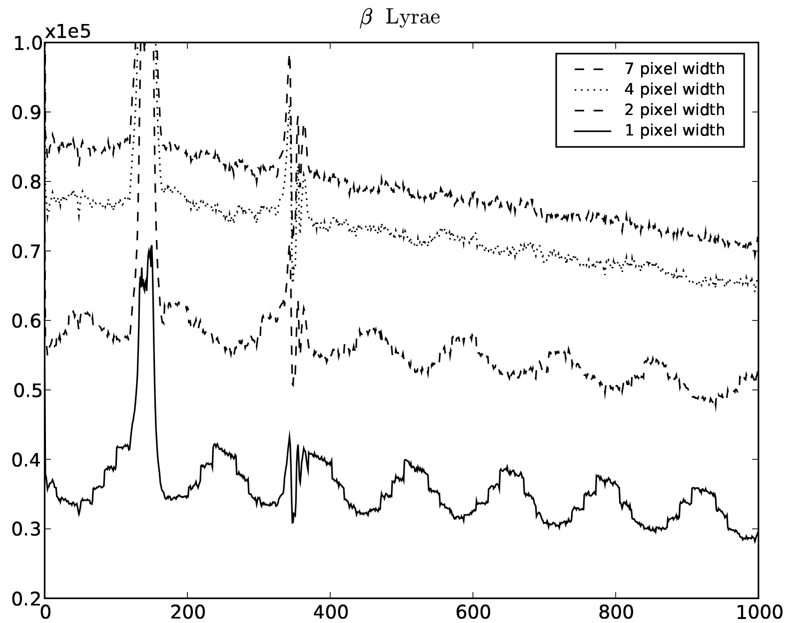

Figure 1: Extracted STIS G750M spectra of the star β Lyrae (exposure rootname o5dh01010) using the standard `calstis` pipeline and various extraction widths as shown in the legend. The unit of the X axis is CCD pixels, and the Y-axis unit is ADU. The scalloped pattern, caused by pixel aliasing, is evident in the uninterpolated spectra.

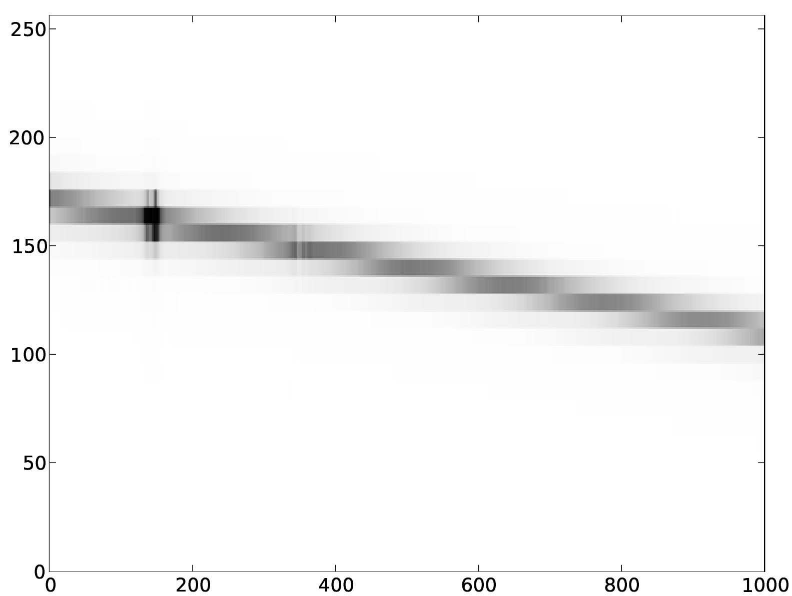

Figure 2: Spectral image of the star whose extracted spectra were shown in Figure 1. The stairstep pattern or aliasing is due to the slightly tilted spectrum and the marginally sampled point spread function. The vertical scale is enlarged to show the aliasing.

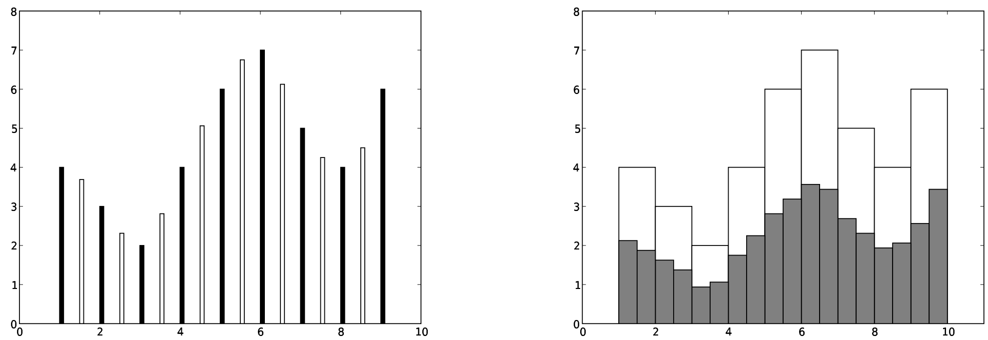

Figure 3: Left panel: Interpolation of data using a 3rd-order polynomial. The original values (filled bars) are located at integral values and the interpolated values (open bars) are at half integral values. Right panel: Average interpolation of data using a 2nd-order polynomial. The original value (white rectangles) span the integers, and the interpolated values (gray rectangles) span the half integers.

difference between adjacent data points is large. Better results can be achieved by using higher (5th or 7th) order polynomials (Figure 3).

Integrating detectors such as CCDs and IR arrays have pixels of finite size. The electrons (or counts) in each pixel are not located at the center of the pixel, but instead are averaged over the area of the pixel. Interpolation — or what we'll call *point-interpolation* — implicitly assumes that the value is located at a point. Instead the underlying function $f(x)$ should be average over the area of the pixel:

$$\lambda_{0,k} = \int_k^{k+1} f(x)dx,$$

where $\lambda_{0,k}$ is the counts in the pixel and k and $k+1$ are the boundaries of the pixel (Figure 3). This is *average-interpolation* and is the most appropriate interpolation for integrating detectors (see e.g. Sweldens 1997, Donoho 1993).

The difference between point-interpolation and average-interpolation may seem minor, but the difference can actually be significant, particularly when accurate fluxes are desired. For astronomical imaging, both interpolation algorithms should give the same total flux for an isolated point source using a sufficiently large extraction region. However, as the extraction region decreases, the measured fluxes will begin to differ. The difference can be $> 50\%$ in some cases with the largest difference occurring where the PSF's gradient is greatest. The reason for this difference is that the distribution of flux within each pixel is different for the two algorithms. This problem becomes more acute when the source is no longer isolated, such as an image of a globular cluster, or the spectrum of an extended source. In this case, the size of the extraction region is limited, possibly by neighboring sources that partially overlap the target. An accurate estimate of the total flux in this case requires an interpolation algorithm that accurately recreates the underlying flux distribution.

3. Wavelets

Wavelets are usually associated with the compression of signals or images by the application of an analysis wavelet (forward transform) of a scaling function. The forward transform uses low and high pass filters to divide the image into smoothed and residual images. The synthesis wavelet is just the inverse transform. It creates a higher resolution image from a coarser image.

Multiresolution is the result of the dilation (or refinement) equation:

$$\phi(t) = \sqrt{2} \sum_{k=0}^{N} c(k)\phi(2t - k),$$

where the scaling function, $\phi(t)$, is a continuous function in t and the coefficients $c(k)$ are discrete in k. This equation relates the scaling function at one scale to the scaling function of the next finer scaler and shows how to calcluate new coefficients that are half way between the old ones. In other words, we can reproduce the scaling function $\phi(t)$ to any resolution by recursion of the dilation equation.

Average-interpolation and (iterative) refinement are two key characteristics of our interpolation algorithm. They ensure that the total counts in a pixel are conserved and the distribution of counts within a subpixel is non-negative. A polynomial is used to approximate the underlying flux distribution. Note that this type of interpolation cannot be done in a single step, i.e. a pixel cannot be subdivided into eight subpixels in one step. Otherwise, there is the possiblity that some subpixels will have negative values, which is not physically possible.

4. Algorithm

The algorithm is a rather simple one-dimensional interpolation problem. The goal is to improve the spatial resolution along the slit (the cross-dispersion direction) in order to reduce the effects of aliasing. We are not interested in improving the spectral resolution, though this is easily achieved by applying this algorithm in the dispersion direction. The partitioning of the counts within each pixel is done by assuming that a N-th order polynomial is a reasonable approximation to the local flux distribution. Average interpolation is used because the CCDs are integrating detectors. Therefore, a polymomial is fit to the cumulative distribution of N-1 pixels, where N is an even integer. The first point of the polynomial is zero, since the integrated area is zero, while the last point is the sum of the N-1 pixels. For each polynomial, only one value, the midpoint of the central pixel, needs to be calculated. Neville's algorithm is used to find this value because it is fast and accurate. The counts in the two subpixels are just the differences between the midpoint value and the points on either side. The algorithm is then repeated for each subpixel until the desired resolution is reached. For STIS three iterations, yielding eight subpixels, usually gives sufficient resolution.

The wavelet algorithm does a very good job of reducing the aliasing, though some may still be present at the few percent level. The aliasing can be reduced further by applying an optional convolution step to the interpolated image. The kernel that is used is an approximation of the instrumental PSF and has the form $(1 + (x/a)^2)^{-2}$, where a is ≈ 1.3 pixels (see also Martin 2004).

5. Results

Figure 4 shows the interpolated image with convolution for three iterations or eight subpixels. The image shows very little of the effects of aliasing. The interpolated spectrum is shown in Figure5 for extraction widths of 1, 2, 4 and 7 pixels. Unlike the uninterpolated spectra, the 1, 2, and 4 pixel width spectra are nearly identical to the 7 pixel width spectrum: only the flux is reduced by a proportional amount.

Figure 6 shows the PSF or cross-dispersion profile for a point source. The black points map the pixel-integrated profile, which is created by shifting the spectral trace so it lies along one row. This causes adjacent pixels in the same row to be shifted slightly with respect to the others, filling in the gaps. The profile is mostly symmetric with wide wings

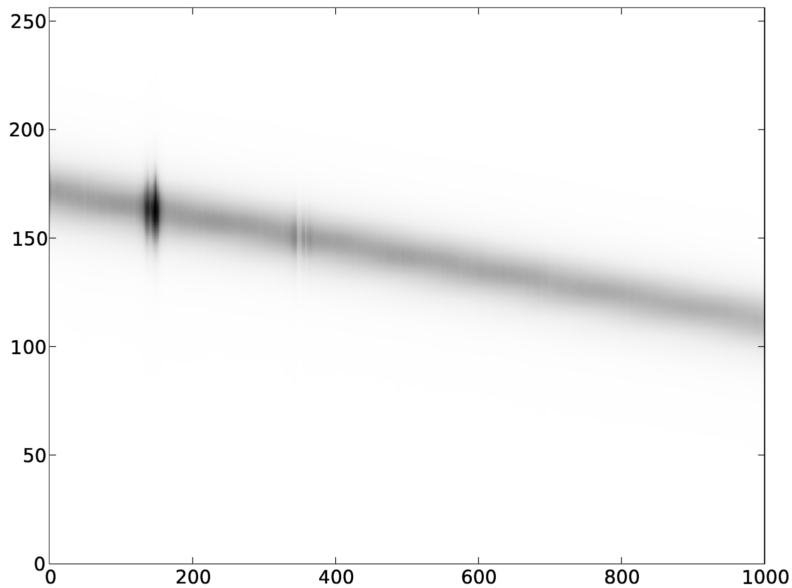

Figure 4: Spectral image of star in Figures 1 and 2 after wavelet interpolation and convolution by the instrumental point spread function.

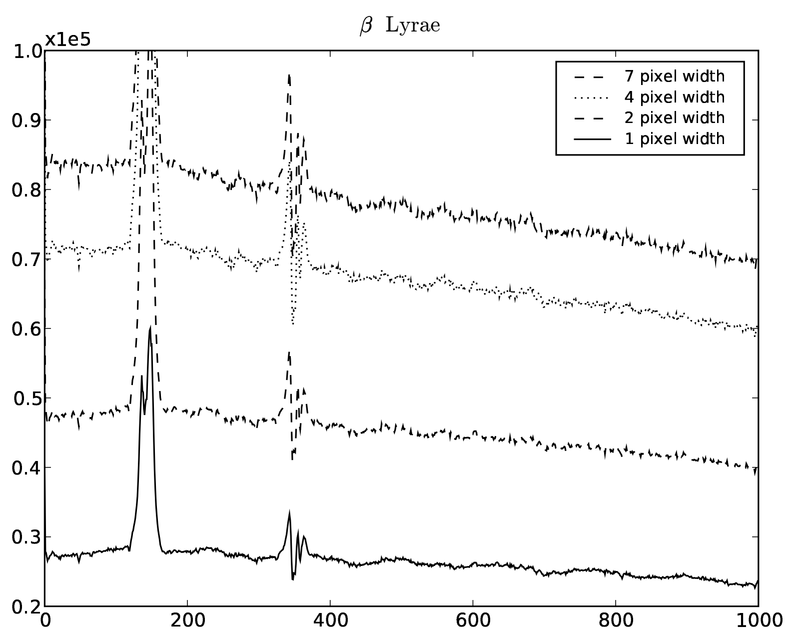

Figure 5: Spectra of star in Figure1 after wavelet interpolation and convolution.

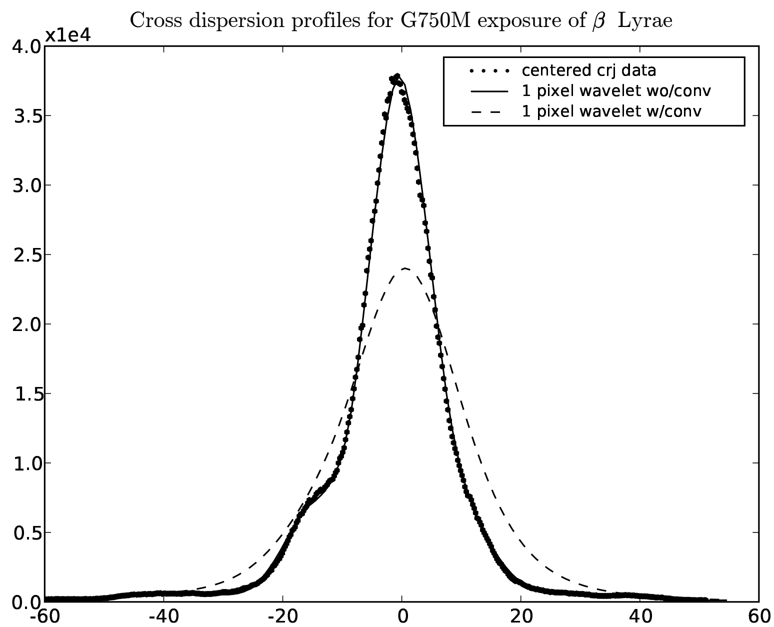

Figure 6: A comparison of the measured pixel-integrated PSF (black points) and the wavelet-interpolated PSF without (solid line) and with (dashed line) convolution.

on each side and a low shoulder on the left side. For comparison, the solid line is the profile along a single column from the interpolated image without convolution. Each point is the sum of eight adjacent subpixels, so that the total area is equal to one pixel as is the case for the black points. A plot of the individual subpixels produces a line that is slightly narrower and more peaked than the pixel integrated profile. The solid line follows the points very closely, except at the peak and near the shoulder. (Note that different columns have different cross-dispersion profiles, depending on the location of the trace: See Figure 9 in Dressel et al. 2006.) The dashed line is the profile from an interpolated image with convolution. This profile is lower and slightly ($\sim 15\%$) broader than the points.

6. Summary

In most situations, interpolation with convolution is the recommended approach. However in situations where the highest spatial resolution is required, such as observations of the binary star WR 140 where the separation of the two stars is about three pixels, interpolation without convolution is preferred, since convolution broadens the image enough to make source confusion a problem. In the case of WR 140, a strong emission line in one stellar spectrum can distort the neighboring spectrum, resulting in incorrect results.

One drawback of this algorithm is that it may become unstable when high order ($N > 5$) polynomials are used for more than three iterations. In this situation we recommend using a lower order polynomial when doing large number of iterations or beginning with a high order polynomial for the first one or two iterations and then switching to a lower order polynomial for succeeding iterations.

This paper has not discussed what errors are associated with the interpolated values. This aspect of the algorithm will be discussed in a forthcoming paper as will the use of finite impulse response (FIR) wavelet filters on image interpolation or deconvolution.

This algorithm is being added as a post-processing task to the CALSTIS package of STSDAS. PEB wishes to thank Paul Goudfrooij for useful suggestions and the opportunity and time to work on this project.

References

Davidson, K. 2004, Technical memo no. 1, Dept. of Astronomy, Univ. of Minnisota, available through `http://etacar.umn.edu/treasury`.

Dressel, L. L. 2003, in Active Galactic Nuclei: from Central Engine to Host Galaxy, S. Collin, F. Combes, & I. Shlosman (San Francisco: Astronomical Society of the Pacific), 393.

Dressel, L. L., Barrett, P. E., Goudfrooij, P., & Hodge, P. E. 2006, this volume, 267

Donoho, D. 1993, Technical Report, Dept. of Statistics, Stanford Univ.

Kim Quijano, J., et al. 2003, "STIS Instrument Handbook", Version 7.0, (Baltimore: STScI), 240.

Martin, J. 2004, Technical memo no. 2, Dept. of Astronomy, Univ. of Minnisota, available through `http://etacar.umn.edu/treasury`.

Sweldens, W. & Schröeder, P. 1995, SIGGRAPH '95 Course Notes: Wavelets and their Applications in Computer Graphics, 3, 76.